Supplementary Material for

A Neutral pH Aqueous Biphasic System Applied to Both Static and Flow Membrane-free Battery

1. FIGURES
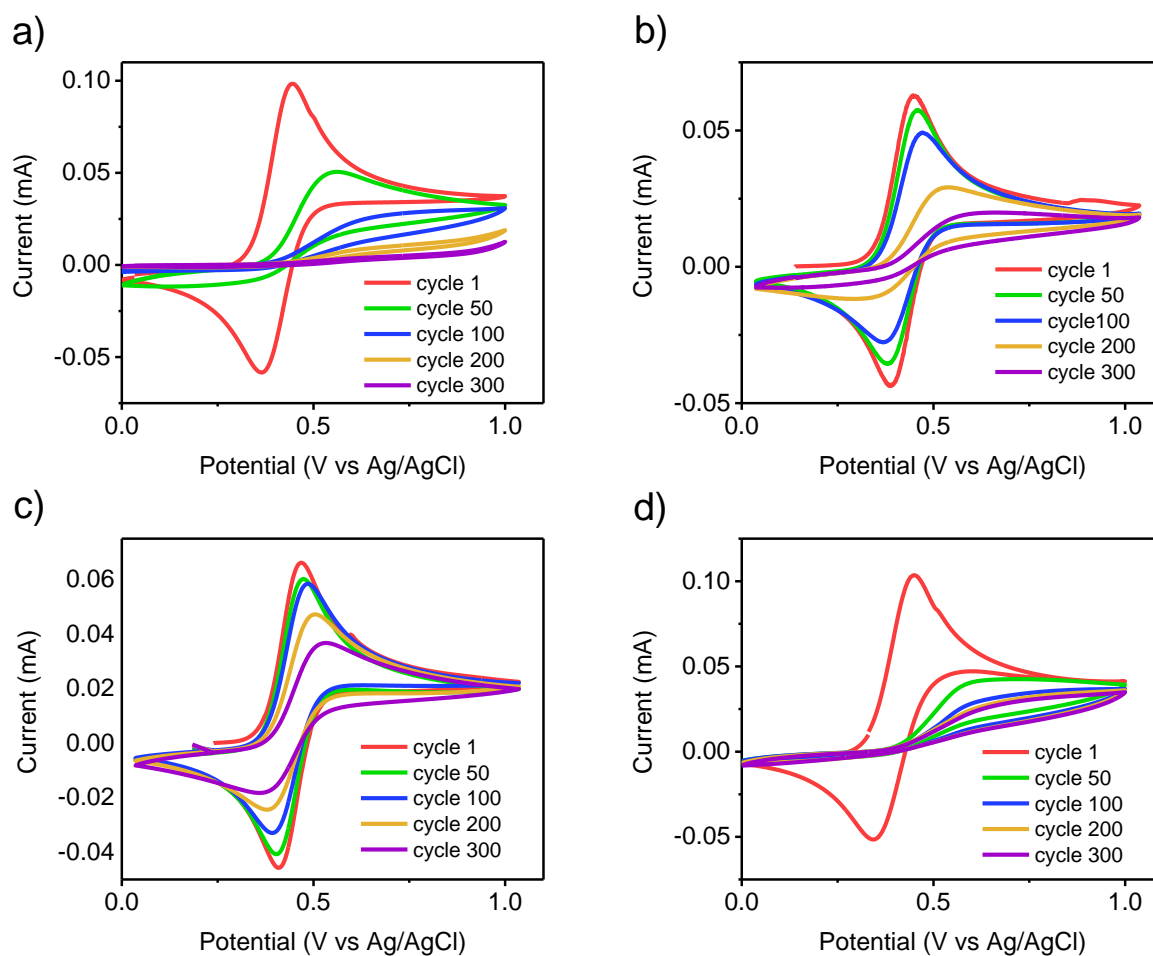

Figure S1. FcNCl electrochemical stability in different supporting electrolytes. CV at 10 mV s^{-1} of a 20 mM FcNCl solution in a) 1 M NaCl; b) 1 M Na$_2$SO$_4$; c) 1 M (NH$_4$)$_2$SO$_4$; d) 1 M NH$_4$Cl.
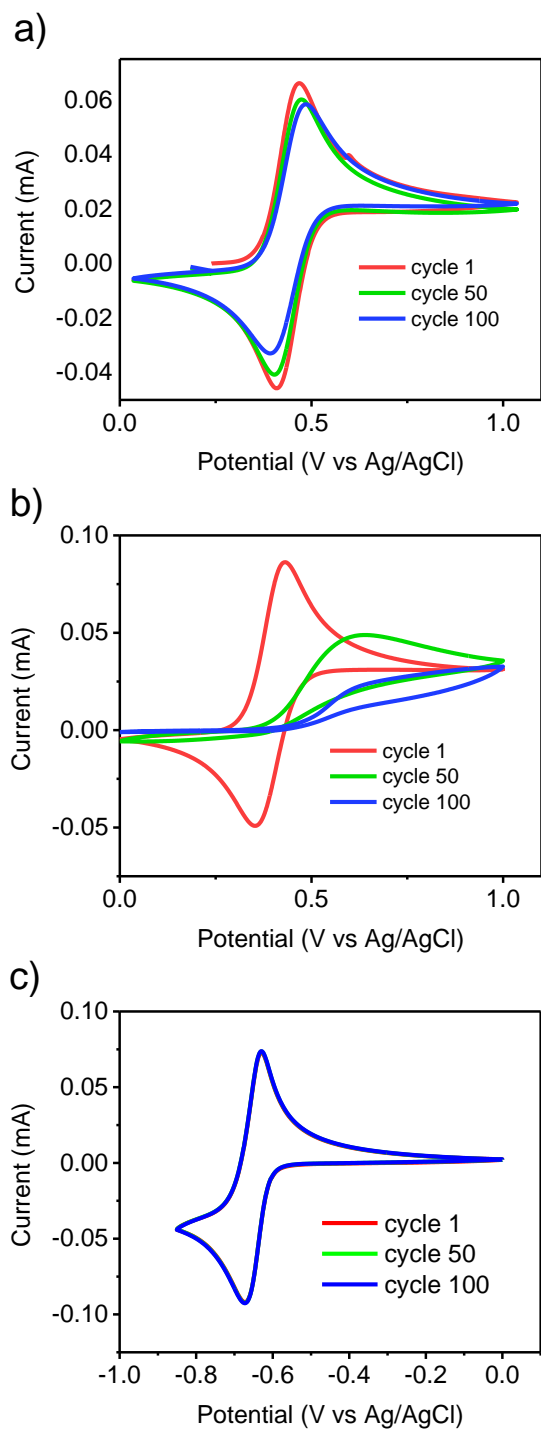
Figure S2. Electrochemical compatibility test between FcNCl and MV. a) 20 mM FcNCl in 1 M $(NH_4)_2SO_4$; b) 20 mM FcNCl and 20 mM MV in 1 M $(NH_4)_2SO_4$ under argon atmosphere; c) Negative potential scan in CV of 20 mM FcNCl and 20 mM MV in 1 M $(NH_4)_2SO_4$. All CV were performed at 10 mVs^{-1} and room temperature. These experiments clearly evidenced that the electrochemistry of FcNCl is drastically affected by the presence of MV whereas the electrochemistry of MV is not affected by the presence of FcNCl
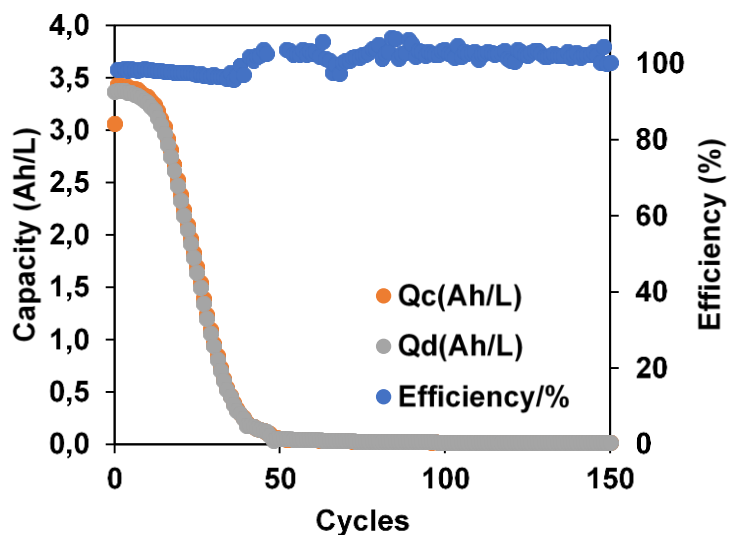
Figure S3. Incompatibility test of FcNCl and MV. Results of a cycling test performed in a conventional filter press flow battery using an anion – exchange membrane AFN (astom corp). (Charge capacity, orange dots; Discharge capacity grey dots; coulombic efficiency, blue dots); Flow rate: 20 mL/min. 100%SOC. Graphite felt electrodes (10 cm^2; 3 mm thickness). Electrolyte composition; 0.15 M FcNCl, 0.15 M MV in 1M $(NH_4)_2SO_4$ electrolyte. Same electrolyte was used as catholyte and anolyte. Electrolytes were purged with argon. Volume electrolyte: 9 mL
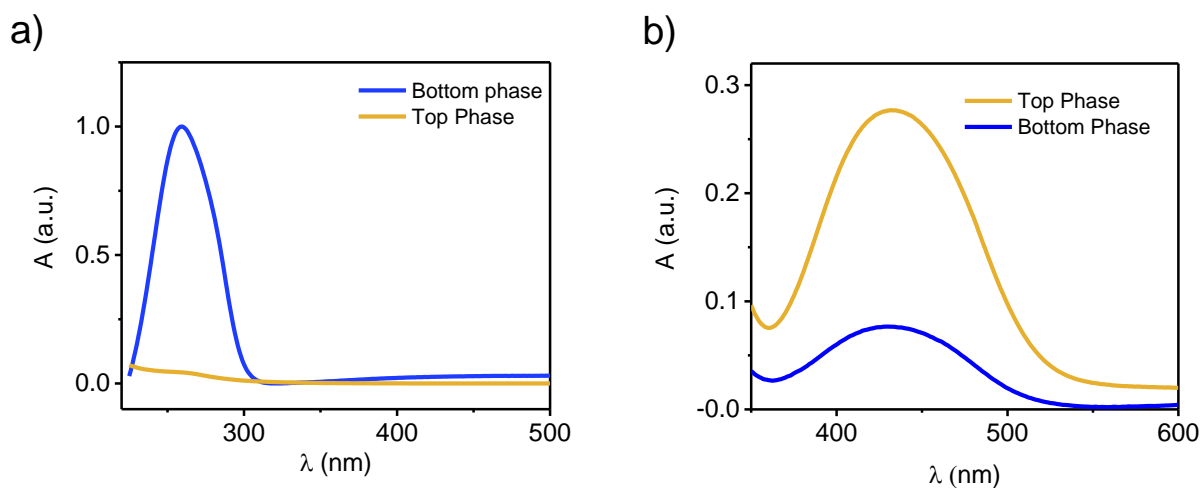
Figure S4. Partition coefficient determination. UV-vis analysis of each phase of the system (top phase in yellow color and bottom phase in blue color). a) UV spectra of the biphasic system containing MV; b) UV spectra of the biphasic system containing FcNCl.
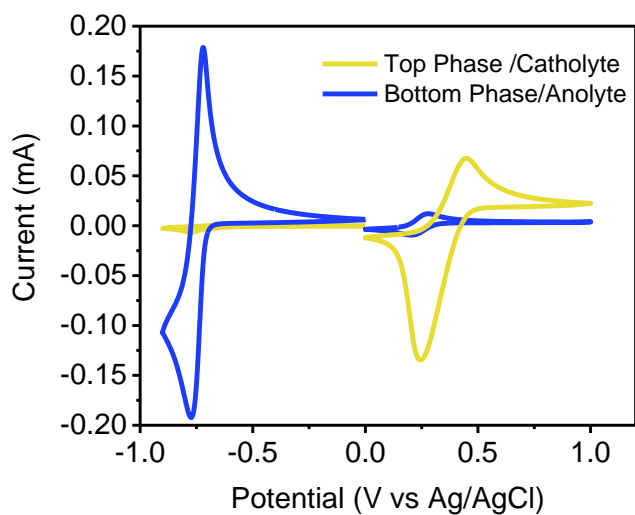

Figure S5. Cyclic voltammetry of top and bottom phase of biphasic system containing 20 mM active species MV and FcNCl at equilibrium. Scan rate 10 mVs^{-1}
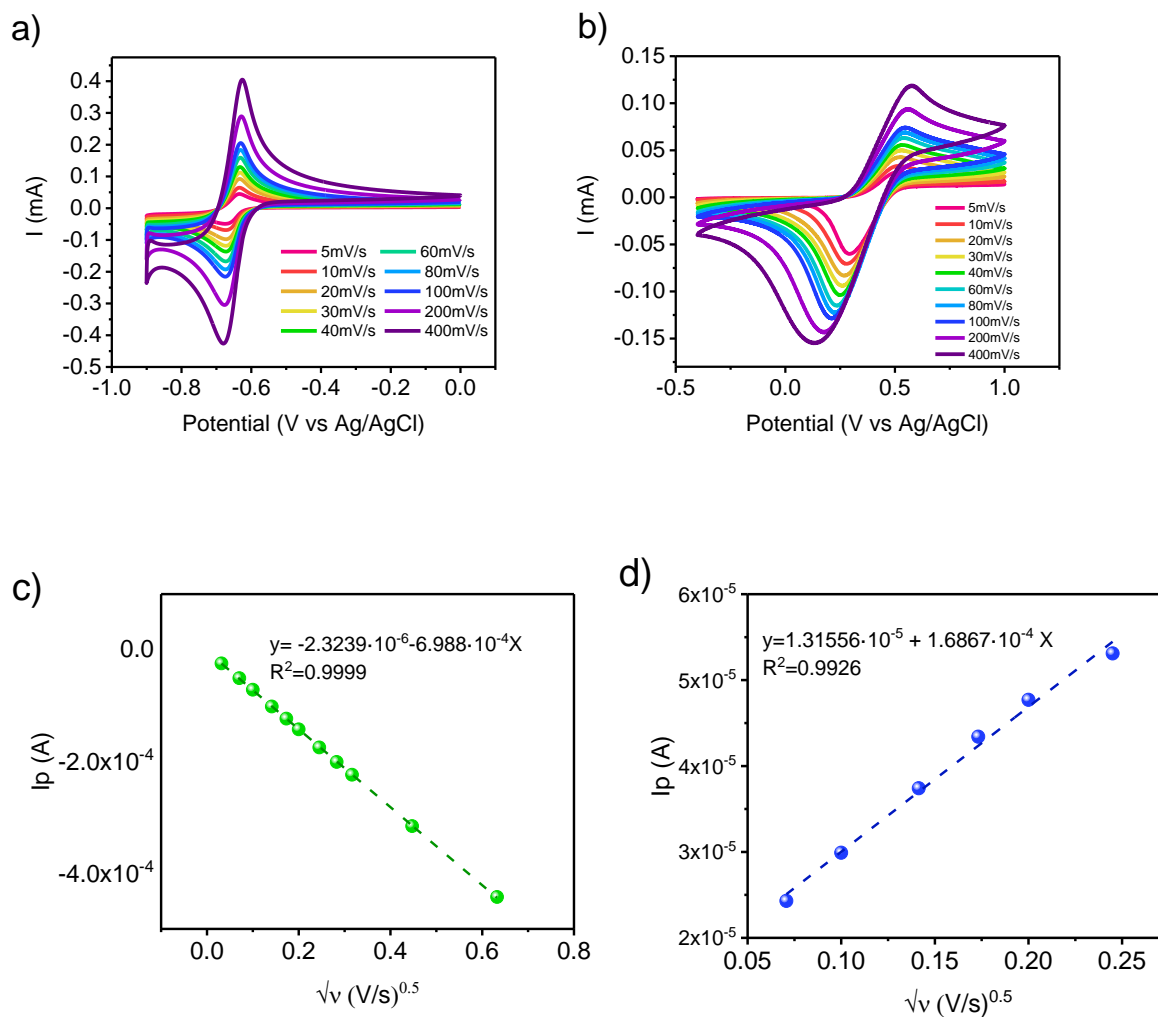
Figure S6. Electrochemical characterization of each electrolyte/phase and diffusion and kinetics parameters calculation. Active species concentration 20 mM. a) and b) cyclic voltammetry at different scan rates of the bottom phase/anolyte and the top phase/catholyte, respectively; c) and d) Peak current versus square root of scan rate for bottom and top phase, respectively.
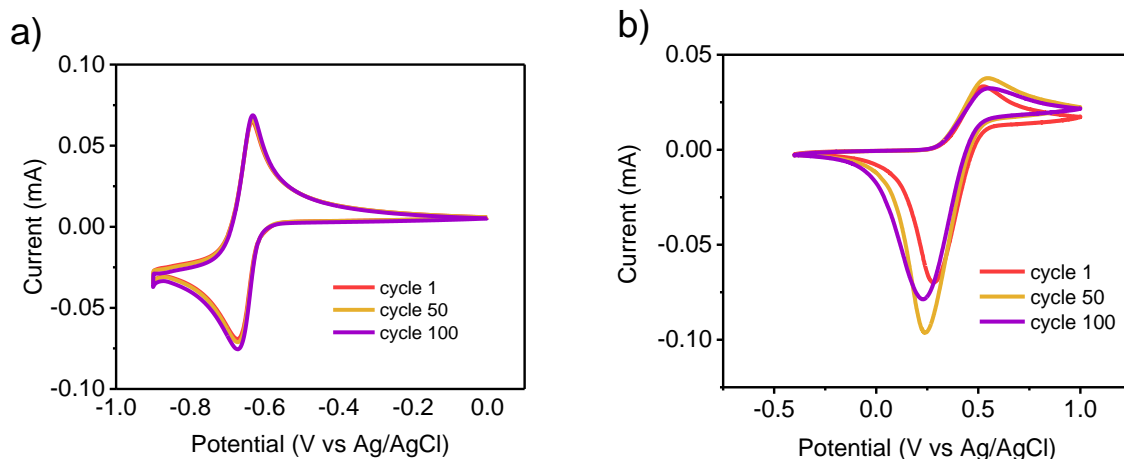
Figure S7. Cycling test of each electrolyte/phase at equilibrium by cyclic voltammetry at 10 mV·s^{-1} and 20 mM active species concentration. a) Bottom phase; b) Top phase
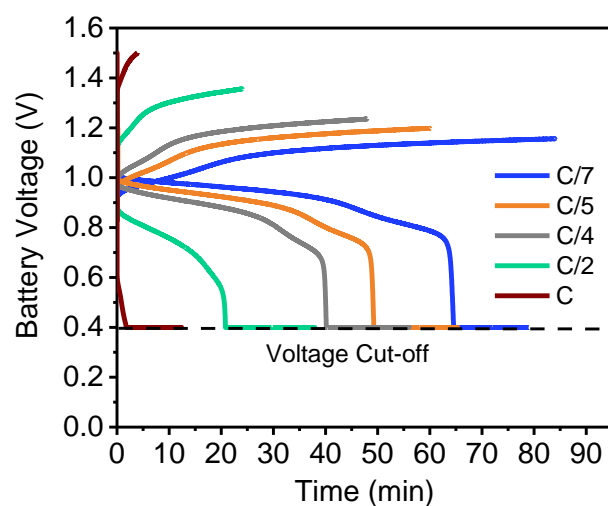

Figure S8. Galvanostatic charge and galvanostatic + potenciostatic discharge voltage profile versus time of more concentrated "static" battery (0.1 M) at different C-rate (20% SOC)
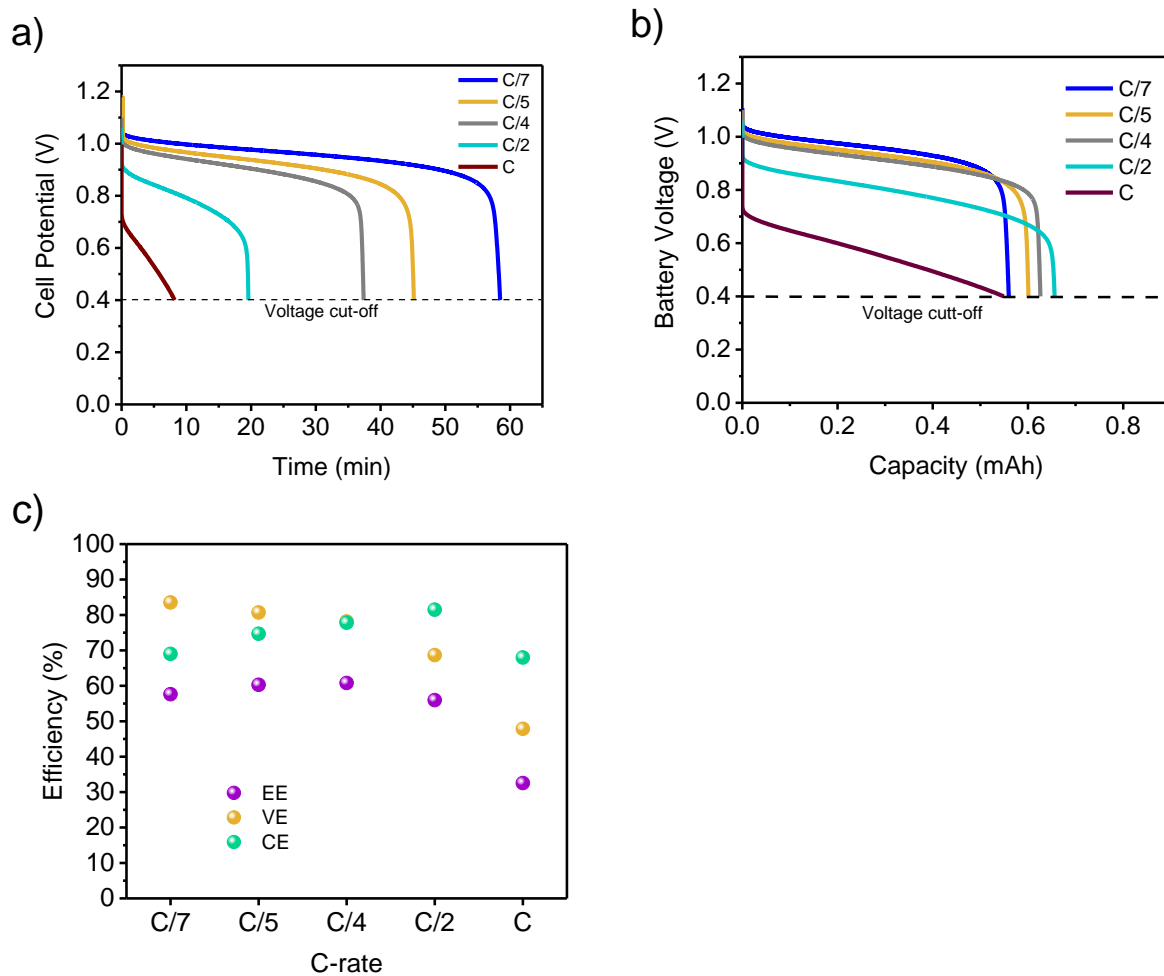
Figure S9. Galvanostatic battery characterization with 0.1 M active species concentration. Charge constant current C/5 and different discharge current. a) Discharge voltage profile at different current densities versus time. b) Discharge voltage profile at different current densities versus capacity. c) Efficiency analysis.
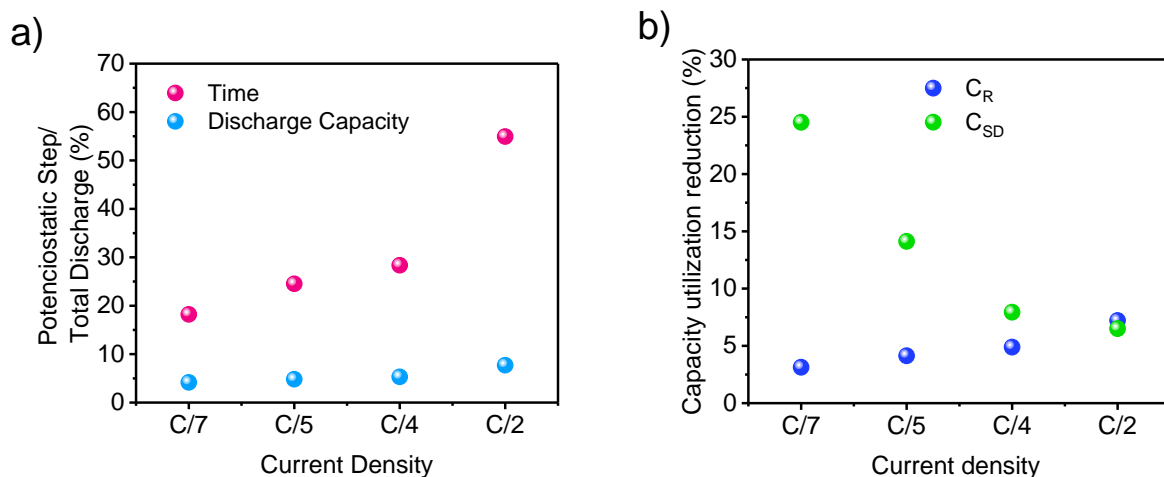
Figure S10. Analysis battery characterized at different current densities (same current for charge and discharge) and 0.1 M active species concentration. a) Analysis of potenciostatic step duration in discharge respect total discharge in terms of time and capacity. b) Capacity not available for discharging due to diffusion limitations (C_R) and self-discharge (C_{SD}) at different current density for a battery that was discharged only galvanostatically.
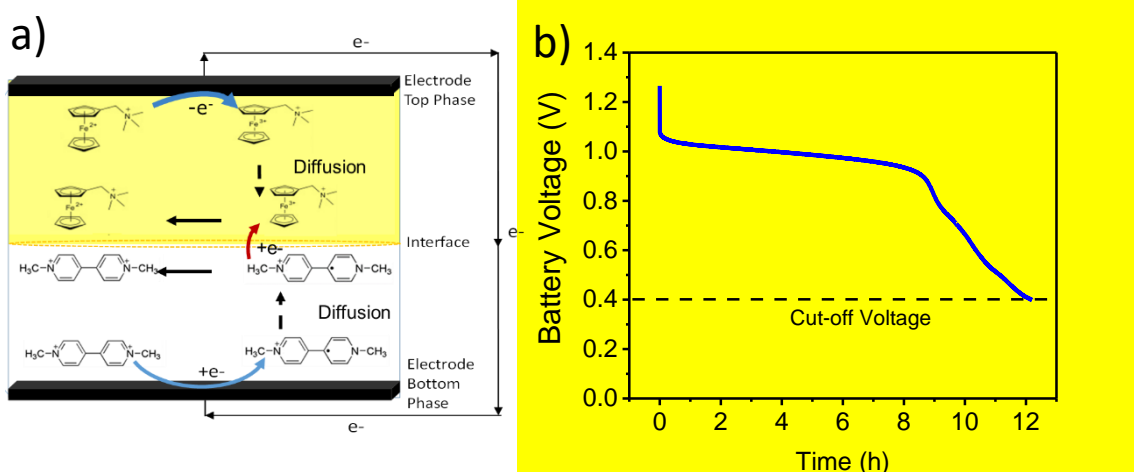
Figure S11. a) Schemed of self discharge mechanism. b) Self-discharge experiment. OCV evolution over time once the battery was charged up to 20%SOC.
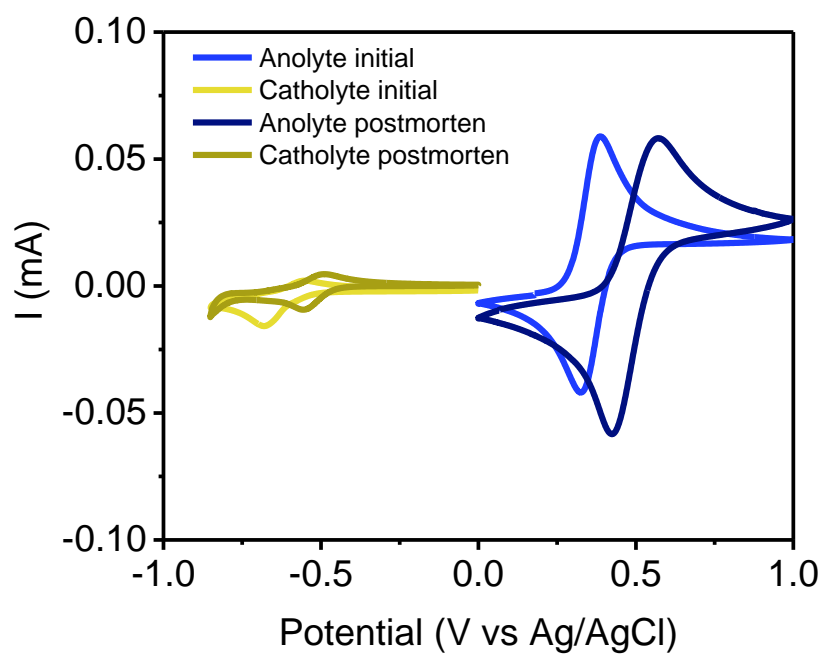
Figure S12. Crossover analysis. Cyclic Voltammetry of Anolyte (blue curves) and Catholyte (yellow curves) at 10 mV·s^{-1} before and after galvanostatic charge/ galvanostatic+ potenciostatic discharge cycling at C/2.

2. TABLES

Table S1. Merchuck parameters obtained from experimental binodal data fitting

Merchuck parameters		Standard error (95% confidence)
A	88.4764	dA=1.2058
B	-0.40237	dB=0.0069032
C	0.00020138	dC=$5.3233 \cdot 10^{-6}$

Table S2. Tie line parameters obtained from the experimental data fitting

Tie line	
TLL	61.8304
α	0.454561

Table S3. Comparison between reported aqueous redox flow batteries with active species from the same families (viologen and trimethylaminoferrocene)
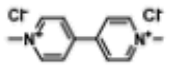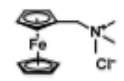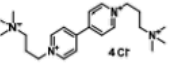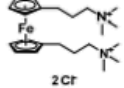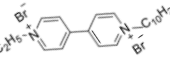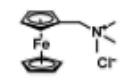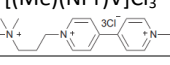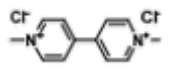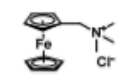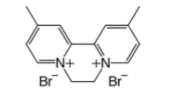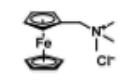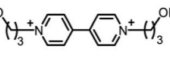
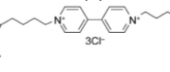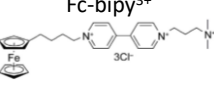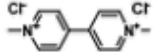| Anolyte	Catholyte	Sup. salt	Species Conc.	OCV (V)	Membrane	Cycles/Current density (mA/cm²)	Capacity Retention (per cycle)/(per day) (%)	Energy density (theoretical)* (Wh/L)	Energy density (max)** (Wh/L)	Merit/limitation	Ref
MV	FcNCl	2 M NaCl	0.7/0.7 M	1.06	Selemion, AEM	500/60	99.958/98.7	9.95	45.5	Neutral pH /reactant stability	[1]
			0.5/0.5 M			700/60	99.987/99.42	7.1			
BTMAP-Vi	BTMAP-Fc	-	1.3/1.3 M	0.75	Selemion, AEM	250/50	99.9943/99.90	13	20	High Stability /low cell voltage	[2]
			0.75/1 M			500/50	99.9989/99.969	8.57			
EDV+HBCD	FcNCl	2 M KCl	0.1/0.11 M	0.97	Selemion, AEM	500/13.33	99.963/97.16	1.36	N.A	Bulk electrolyte stability/low current density	[3]
$[(Me)(NPr)V]Cl_3$	FcNCl	2 M NaCl	0.25/0.5 M	1.38	Selemion, AEM	50/60	99.82/N.A	12.32	79.5	Two electrons anolyte/shorter cycling test	[4]
$[(NPr)_2V]Br_4$				1.33		100/60	99.99/N.A	11.88	68.1		
MV	FcNCl	2 M NaCl	0.5/0.5 M	1.06	Selemion, AEM	200/60	99.988/N.A	7.1	45.5	Effect different thickness AEM/reactant stability	[5]
		2 M KCl					99.971/N.A				
Diquat	FcNCl	1.5 M NaCl	0.5/0.5 M	1.12	Selemion, AEM	100/5	99.8/N.A	7.5	30.02	High theoretical Edensity/poor current density	[6]
BHOP-Vi	FcNCl	water	2/1.5 M	1	Selemion DSV	100/100	99.9995/98.872	30.63	N.A	No sup. Electrolyte/cap loss (degradation & crossover)	[7]
		1 M NaCl	0.1/0.1 M			300/40	99.982/98.35	1.34			
Fc-bipy^{3+}	Fc-bipy^{3+}	1 M NaCl	0.5/0.5 M	0.7	Selemion, AEM	4000/10 (static)	99.99375/99.75	4.69	N.A	Symmetric cell/ Using membrane & low current density	[8]

Table S3 (continuation). Comparison between reported aqueous redox flow batteries with active species from the same families (viologen and trimethylaminoferrocene)
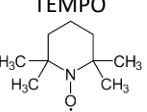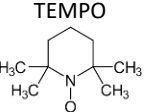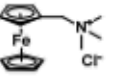
Anolyte	Catholyte	Sup. salt	Species Conc.	Cell Voltage (V)	Membrane	Cycles /Current density (mA/cm²)	Capacity Retention (per cycle) /(per day) (%)	Energy density (theoretical)* (Wh/L)	Energy density (max)** (Wh/L)	Merit/limitation	Ref
MV	FcNCl	PEG$_{1000}$ (NH$_4$)$_2$SO$_4$	0.1/0.1 M	1.1	NO	250/1.2 (static)	99.83/97.51	1.475	21.7	No separator, thermodynamic separation/ selfdischarge	This work
						250/ 1.25 (static)	100$^{\#}$				
						100/2.8 (flow)	99.838/95.993-100$^{\#}$				

*considering used active species concentration; **considering active species solubility limit; #: considering potentiostatic step.
MV: methyl viologen dichloride; FcNCl: (ferrocenylmethyl)trimethylammonium chloride; BTMAP-Vi: bis(3-trimethylammonio)propyl viologen tetrachloride; BTMAP-Fc: bis((3-trimethylammonio)propyl)ferrocene dichloride; EDV: 1-Decyl-1'-ethyl-4,4'-bipyridinium dibromide; HBCD: (2-hydroxypropyl)-β-cyclodextrin. Diquat: derivative of 2,2'-bipyridylium. BHOP-Vi=1,1'-bis(3-hydroxypropyl) viologen dibromide; Fc-bipy3+ :

Table S4. Comparison between reported totally aqueous membrane-free batteries

Anolyte	Catholyte	Sup. salt	Species Conc.	OCV (V)	Membrane	Cycles /Current density (mA/cm²)	Coulombic efficiency (%)	Capacity Retention (per cycle)	Depth of discharge (DoD) (%)	Energy density (max)** (Wh/L)	Merit/ limitation	Ref
MV	TEMPO	Biphasic system IL+Na$_2$SO$_4$	0.02/0.02 M	1.35	NO	20/0.16 (static)	70	100	5	N.A	Neutral pH & high voltage /reactant concentration	[9]
MV	TEMPO	Biphasic system PEG$_{1000}$ + Na$_2$SO$_4$	0.1/0.1 M	1.25	NO	550/3 (static)	82	99.99	5	1.6	Safe sup. electrolyte/ low Depth discharge	[10]
MV	FcNCl	Biphasic system PEG$_{1000}$ + (NH$_4$)$_2$SO$_4$	0.1/0.1 M	1.1	NO	200/0.45 (static)	88.8	89	20	21.7	Flow operation/ low current density	This work
						250/ 1.25 (static)	95.8*	100				
						100/2.8 (flow)	93.8*	100				

*Galvanostatic-potentiostatic discharge **considering active species solubility limit
IL: tributyltetradecylphosphonium chloride; MV: methyl viologen dichloride; FcNCl: (ferrocenylmethyl)trimethylammonium chloride; TEMPO: 2,2,6,6-Tetramethylpiperidin-1-yl)oxyl.

References

[1]   B. Hu, C. DeBruler, Z. Rhodes, T.L. Liu, Long-Cycling Aqueous Organic Redox Flow Battery (AORFB) toward Sustainable and Safe Energy Storage, J. Am. Chem. Soc. 139 (2017) 1207–1214. https://doi.org/10.1021/jacs.6b10984.

[2]   E.S. Beh, D. De Porcellinis, R.L. Gracia, K.T. Xia, R.G. Gordon, M.J. Aziz, A neutral pH aqueous organic- organometallic redox flow battery with extremely high capacity retention, ACS Energy Lett. 2 (2017) 639–644. https://doi.org/10.1021/acsenergylett.7b00019.

[3]   A. Korshunov, A. Gibalova, M. Grünebaum, B.J. Ravoo, M. Winter, I. Cekic-Laskovic, Host-Guest Interactions Enhance the Performance of Viologen Electrolytes for Aqueous Organic Redox Flow Batteries, Batter. Supercaps. 4 (2021) 923–928. https://doi.org/10.1002/batt.202100018.

[4]   C. DeBruler, B. Hu, J. Moss, X. Liu, J. Luo, Y. Sun, T.L. Liu, Designer Two-Electron Storage Viologen Anolyte Materials for Neutral Aqueous Organic Redox Flow Batteries, Chem. 3 (2017) 961–978. https://doi.org/10.1016/j.chempr.2017.11.001.

[5]   B. Hu, C. Seefeldt, C. Debruler, T.L. Liu, Boosting the energy efficiency and power performance of neutral aqueous organic redox flow batteries, J. Mater. Chem. A. 5 (2017) 22137–22145. https://doi.org/10.1039/c7ta06573f.

[6]   J. Huang, Z. Yang, V. Murugesan, E. Walter, A. Hollas, B. Pan, R.S. Assary, I.A. Shkrob, X. Wei, Z. Zhang, Spatially Constrained Organic Diquat Anolyte for Stable Aqueous Flow Batteries, ACS Energy Lett. 3 (2018) 2533–2538. https://doi.org/10.1021/acsenergylett.8b01550.

[7]   Y. Liu, Y. Li, P. Zuo, Q. Chen, G. Tang, P. Sun, Z. Yang, T. Xu, Screening Viologen Derivatives for Neutral Aqueous Organic Redox Flow Batteries, ChemSusChem. 13 (2020) 2245–2249. https://doi.org/10.1002/cssc.202000381.

[8]   Y. Zhu, F. Yang, Z. Niu, H. Wu, Y. He, H. Zhu, J. Ye, Y. Zhao, X. Zhang, Enhanced cyclability of organic redox flow batteries enabled by an artificial bipolar molecule in neutral aqueous electrolyte, J. Power Sources. 417 (2019) 83–89. https://doi.org/10.1016/j.jpowsour.2019.02.021.

[9]   P. Navalpotro, C.M.S.S. Neves, J. Palma, M.G. Freire, J.A.P. Coutinho, R. Marcilla, Pioneering Use of Ionic Liquid-Based Aqueous Biphasic Systems as Membrane-Free Batteries, Adv. Sci. 5 (2018) 1–10. https://doi.org/10.1002/advs.201800576.

[10]   P. Navalpotro, C. Trujillo, I. Montes, C.M.S.S. Neves, J. Palma, M.G. Freire, J.A.P. Coutinho, R. Marcilla, Critical aspects of membrane-free aqueous battery based on two immiscible neutral electrolytes, Energy Storage Mater. 26 (2020) 400–407. https://doi.org/10.1016/j.ensm.2019.11.011.